

**Technical Justification for
Eliminating Large Primary Loop
Pipe Rupture as the Structural
Design Basis for the H. B. Robinson
Unit 2 Nuclear Power Plant for the
License Renewal Program**

WCAP-15628-NP Revision 0

Technical Justification for Eliminating Large Primary Loop Pipe Rupture as the Structural Design Basis for the H. B. Robinson Unit 2 Nuclear Power Plant for the License Renewal Program


D. C. Bhowmick

April 2003

Verifier:


J. F. Petsche

Approved:


S. A. Swamy, Manager
Structural Mechanics Technology

Westinghouse Electric Company LLC
P.O. Box 355
Pittsburgh, PA 15230-0355

©2003 Westinghouse Electric Company LLC
All Rights Reserved

TABLE OF CONTENTS

	EXECUTIVE SUMMARY	ix
1.0	INTRODUCTION	1-1
1.1	PURPOSE	1-1
1.2	BACKGROUND INFORMATION	1-1
1.3	SCOPE AND OBJECTIVES	1-2
1.4	REFERENCES	1-3
2.0	OPERATION AND STABILITY OF THE REACTOR COOLANT SYSTEM	2-1
2.1	STRESS CORROSION CRACKING	2-1
2.2	WATER HAMMER	2-2
2.3	LOW CYCLE AND HIGH CYCLE FATIGUE	2-2
2.4	REFERENCES	2-3
3.0	PIPE GEOMETRY AND LOADING	3-1
3.1	INTRODUCTION TO METHODOLOGY	3-1
3.2	CALCULATION OF LOADS AND STRESSES	3-1
3.3	LOADS FOR LEAK RATE EVALUATION	3-2
3.4	LOAD COMBINATION FOR CRACK STABILITY ANALYSES	3-3
3.5	REFERENCES	3-3
4.0	MATERIAL CHARACTERIZATION	4-1
4.1	PRIMARY LOOP PIPE AND FITTINGS MATERIALS	4-1
4.2	TENSILE PROPERTIES	4-1
4.3	FRACTURE TOUGHNESS PROPERTIES	4-2
4.4	REFERENCES	4-4
5.0	CRITICAL LOCATIONS AND EVALUATION CRITERIA	5-1
5.1	CRITICAL LOCATIONS	5-1
5.2	FRACTURE CRITERIA	5-1
6.0	LEAK RATE PREDICTIONS	6-1
6.1	INTRODUCTION	6-1
6.2	GENERAL CONSIDERATIONS	6-1
6.3	CALCULATION METHOD	6-1
6.4	LEAK RATE CALCULATIONS	6-2
6.5	REFERENCES	6-2
7.0	FRACTURE MECHANICS EVALUATION	7-1
7.1	LOCAL FAILURE MECHANISM	7-1
7.2	GLOBAL FAILURE MECHANISM	7-1
7.3	RESULTS OF CRACK STABILITY EVALUATION	7-3
7.4	REFERENCES	7-4
8.0	FATIGUE CRACK GROWTH ANALYSIS	8-1
8.1	REFERENCES	8-4
9.0	ASSESSMENT OF MARGINS	9-1
10.0	CONCLUSIONS	10-1
	APPENDIX A LIMIT MOMENT	A-1

LIST OF TABLES

Table	Title	Page
Table 3-1	Dimensions, Normal Loads and Normal Stresses for H. B. Robinson Unit 2	3-4
Table 3-2	Faulted Loads and Stresses for H. B. Robinson Unit 2	3-5
Table 4-1	Measured Tensile Properties (psi) for H. B. Robinson Unit 2 Primary Loop Pipes.....	4-6
Table 4-2	Measured Tensile Properties (psi) for H. B. Robinson Unit 2 Primary Loop Elbows	4-7
Table 4-3	Mechanical Properties for H. B. Robinson Unit 2 Materials at Operating Temperatures.....	4-8
Table 4-4	Chemistry and Fracture Toughness Properties of the Cast Material Heats of H. B. Robinson Unit 2	4-9
Table 4-5	Fracture Toughness Properties for H. B. Robinson Unit 2 Primary Loops for Leak-Before-Break Evaluation at Critical Locations	4-10
Table 6-1	Flaw Sizes Yielding a Leak Rate of 10 gpm at the Governing Locations.....	6-3
Table 7-1	Stability Results for H. B. Robinson Unit 2 Based on Elastic-Plastic J-Integral Evaluations	7-5
Table 7-2	Stability Results for H. B. Robinson Unit 2 Based on Limit Load	7-5
Table 8-1	Summary of Reactor Vessel Transients	8-5
Table 8-2	Fatigue Crack Growth at RPV Inlet Nozzle Safe-End Region (40 and 60 years).....	8-7
Table 8-3	Fatigue Crack Growth at RPV Outlet Nozzle Safe-End Region (40 and 60 years).....	8-7
Table 9-1	Leakage Flaw Sizes, Critical Flaw Sizes and Margins for H. B. Robinson Unit 2.	9-2

LIST OF FIGURES

Figure	Title	Page
3-1	Hot Leg Coolant Pipe.....	3-6
3-2	Schematic Diagram of H. B. Robinson Unit 2 Primary Loop Showing Weld Locations.....	3-7
4-1	Representative Lower Bound True Stress - True Strain Curve for A351 CF8M at 620°F	4-11
4-2	Representative Lower Bound True Stress - True Strain Curve for A351 CF8M at 554°F	4-12
4-3	Pre-Service J. vs. Δa for SA351 CF8M Cast Stainless Steel at 600°F	4-13
6-1	Analytical Predictions of Critical Flow Rates of Steam-Water Mixtures	6-4
6-2	[] ^{a,c,e} Pressure Ration as a Function of L/D.....	6-5
6-3	Idealized Pressure Drop Profile through a Postulated Crack	6-6
7-1	[] ^{a,c,e} Stress Distribution	7-6
7-2	Critical Flaw Size Prediction - Hot Leg at Location 1	7-7
7-3	Critical Flaw Size Prediction - Hot Leg at Location 3.....	7-8
7-4	Critical Flaw Size Prediction - Cross-over Leg at Location 6.....	7-9
7-5	Critical Flaw Size Prediction - Cold Leg at Location 13.....	7-10
8-1	Typical cross-section of RPV Inlet and outlet Nozzle Safe-End.....	8-8
8-2	Reference Fatigue Crack Growth Curves for Carbon and Low Alloy Ferritic Steels	8-9
8-3	Reference Fatigue Crack Growth Curves for Stainless steel in Air Environments	8-10
8-4	Crack Growth Model for Alloy in PWR Environments with Available Data	8-11
A-1	Pipe with a Through-Wall Crack in Bending.....	A-2

EXECUTIVE SUMMARY

The original structural design basis of the reactor coolant system for the Carolina Power and Light Co. H. B. Robinson Unit 2 Nuclear Power Plant required consideration of dynamic effects resulting from pipe break and that protective measures for such breaks be incorporated into the design. Subsequent to the original H. B. Robinson Unit 2 design, an additional concern of Asymmetric Blowdown loads was raised as described in Unresolved Safety Issue A-2 (Asymmetric Blowdown Loads on the Reactor Coolant System). H. B. Robinson Unit 2 Nuclear Power Plant was part of the utilities, which sponsored Westinghouse to resolve the A-2 issue. Generic analyses by Westinghouse to resolve the A-2 issue was approved by the NRC and documented in Generic Letter 84-04 (Reference 1-2).

The approved Westinghouse Generic Analyses were indicated to be directly applicable to H. B. Robinson Unit 2 in Reference 1-2.

Research by the NRC and industry coupled with operating experience determined that safety could be negatively impacted by placement of pipe whip restraints on certain systems. As a result, NRC and industry initiatives resulted in demonstrating that Leak-before-break (LBB) criteria can be applied to reactor coolant system piping based on fracture mechanics technology and material toughness.

Subsequently, the NRC modified 10CFR50 General Design Criterion 4, and published in the Federal Register (Vol. 52, No. 207) on October 27, 1987 its final rule, "Modification of General Design Criterion 4 Requirements for Protection against Dynamic Effects of Postulated Pipe Ruptures (Reference 1-3)." This change to the rule allows use of leak-before-break technology for excluding from the design basis the dynamic effects of postulated ruptures in primary coolant loop piping in pressurized water reactors (PWRs).

This report demonstrates compliance with LBB technology for the H. B. Robinson Unit 2 reactor coolant system piping based on a plant specific analysis for the License Renewal Program. The report documents the plant specific geometry, loading, and material properties used in the fracture mechanics evaluation. Mechanical properties were determined at operating temperatures. Since the piping systems include cast stainless steel, fracture toughness considering thermal aging was determined for each heat of material.

Based on loading, pipe geometry and fracture toughness considerations, enveloping critical locations were determined at which leak-before-break crack stability evaluations were made. Through-wall flaw sizes were postulated which would cause a leak at a rate of ten (10) times the leakage detection system capability of the plant. Large margins for such flaw sizes were demonstrated against flaw instability. Finally, fatigue crack growth was shown not to be an issue for the primary loops.

It is concluded that the Leak-Before-Break conditions are satisfied for the H. B. Robinson Unit 2 primary loop piping. All the recommended margins are satisfied. It is therefore concluded that dynamic effects of RCS primary loop pipe breaks need not be considered in the structural design basis of the H. B. Robinson Unit 2 Nuclear Power Plant for the License Renewal Program.

1.0 INTRODUCTION

1.1 PURPOSE

This report applies to the H. B. Robinson Unit 2 Reactor Coolant System (RCS) primary loop piping. It is intended to demonstrate that for the specific parameters of the H. B. Robinson Unit 2 Nuclear Power Plant, RCS primary loop pipe breaks need not be considered in the structural design basis. The Nuclear Regulatory Commission (NRC) (Reference 1-3) has accepted the approach taken.

1.2 BACKGROUND INFORMATION

Westinghouse has performed considerable testing and analysis to demonstrate that RCS primary loop pipe breaks can be eliminated from the structural design basis of all Westinghouse plant. The concept of eliminating pipe breaks in the RCS primary loop was first presented to the NRC in 1978 in WCAP-9283 (Reference 1-4). That topical report employed a deterministic fracture mechanics evaluation and a probabilistic analysis to support the elimination of RCS primary loop pipe breaks. That approach was then used as a means of addressing Generic Issue A-2 and Asymmetric LOCA Loads.

Westinghouse performed additional testing and analysis to justify the elimination of RCS primary loop pipe breaks. This material was provided to the NRC along with Letter Report NS-EPR-2519 (Reference 1-5).

The NRC funded research through Lawrence Livermore National Laboratory (LLNL) to address this same issue using a probabilistic approach. As part of the LLNL research effort, Westinghouse performed extensive evaluations of specific plant loads, material properties, transients, and system geometries to demonstrate that the analysis and testing previously performed by Westinghouse and the research performed by LLNL applied to all Westinghouse plant (References 1-6 and 1-7). The results from the LLNL study were released at a March 28, 1983, ACRS Subcommittee meeting. These studies, which are applicable to all Westinghouse plant east of the Rocky Mountains, determined the mean probability of a direct LOCA (RCS primary loop pipe break) to be 4.4×10^{-12} per reactor year and the mean probability of an indirect LOCA to be 10^{-7} per reactor year. Thus, the results previously obtained by Westinghouse (Reference 1-4) were confirmed by an independent NRC research study.

Based on the studies by Westinghouse, LLNL, the ACRS, and the AIF, the NRC completed a safety review of the Westinghouse reports submitted to address asymmetric blowdown loads that result from a number of discrete break locations on the PWR primary systems. The NRC Staff evaluation (Reference 1-2) concludes that an acceptable technical basis has been provided so that asymmetric blowdown loads need not be considered for those plant that can demonstrate the applicability of the modeling and conclusions contained in the Westinghouse response or can provide an equivalent fracture mechanics demonstration of the primary coolant loop integrity. In a more formal recognition of Leak-Before-Break (LBB) methodology applicability for PWRs, the NRC appropriately modified 10 CFR 50, General Design Criterion 4,

"Requirements for Protection Against Dynamic Effects for Postulated Pipe Rupture"
(Reference 1-3).

1.3 SCOPE AND OBJECTIVES

The general purpose of this investigation is to demonstrate leak-before-break for the primary loops in H. B. Robinson Unit 2 on a plant specific basis. The recommendations and criteria proposed in Reference 1-8 are used in this evaluation. These criteria and resulting steps of the evaluation procedure can be briefly summarized as follows:

1. Calculate the applied loads. Identify the locations at which the highest stress occurs.
2. Identify the materials and the associated material properties.
3. Postulate a surface flaw at the governing locations. Determine fatigue crack growth. Show that a through-wall crack will not result.
4. Postulate a through-wall flaw at the governing locations. The size of the flaw should be large enough so that the leakage is assured of detection with margin using the installed leak detection equipment when the pipe is subjected to normal operating loads. A margin of 10 is demonstrated between the calculated leak rate and the leak detection capability.
5. Using faulted loads, demonstrate that there is a margin of at least 2 between the leakage flow size and the critical flow size.
6. Review the operating history to ascertain that operating experience has indicated no particular susceptibility to failure from the effects of corrosion, water hammer or low and high cycle fatigue.
7. For the materials actually used in the plant, provide the properties including toughness and tensile test data. Evaluate long term effects such as thermal aging.
8. Demonstrate margin on applied load.

This report provides a fracture mechanics demonstration of primary loop integrity for the H. B. Robinson Unit 2 Plant consistent with the NRC position for exemption from consideration of dynamic effects.

Several computer codes are used in the evaluations. The computer programs are under Configuration Control, which has, requirements conforming to NRC's Standard Review Plan 3.9.1 (Reference 1-9). The fracture mechanics calculations are independently verified (benchmarked).

1.4 REFERENCES

- 1-1 WCAP-7211, Revision 4, "Proprietary Information and Intellectual Property Management Policies and Procedures," January 2001.
- 1-2 USNRC Generic Letter 84-04, Subject "Safety Evaluation of Westinghouse Topical Reports Dealing with Elimination of Postulated Pipe Breaks in PWR Primary Main Loops," February 1, 1984.
- 1-3 Nuclear Regulatory Commission, 10 CFR 50, Modification of General Design Criteria 4 Requirements for Protection Against Dynamic Effects of Postulated Pipe Ruptures, Final Rule, Federal Register/Vol. 52, No. 207/Tuesday, October 27, 1987/Rules and Regulations, pp. 41288-41295.
- 1-4 WCAP-9283, "The Integrity of Primary Piping Systems of Westinghouse Nuclear Power Plant During Postulated Seismic Events," March 1978.
- 1-5 Letter Report NS-EPR-2519, Westinghouse (E. P. Rahe) to NRC (D. G. Eisenhut), Westinghouse Proprietary Class 2, November 10, 1981.
- 1-6 Letter from Westinghouse (E. P. Rahe) to NRC (W. V. Johnston) dated April 25, 1983.
- 1-7 Letter from Westinghouse (E. P. Rahe) to NRC (W. V. Johnston) dated July 25, 1983.
- 1-8 Standard Review Plan: Public Comments Solicited; 3.6.3 Leak-Before-Break Evaluation Procedures; Federal Register/Vol. 52, No. 167/Friday August 28, 1987/Notices, pp. 32626-32633.
- 1-9 Nuclear Regulatory Commission, Standard Review Plan Section 3.9.1, "Special Topics for Mechanical Component," NUREG-0800, Revision 2, July 1981.

2.0 OPERATION AND STABILITY OF THE REACTOR COOLANT SYSTEM

2.1 STRESS CORROSION CRACKING

The Westinghouse reactor coolant system primary loops have an operating history that demonstrates the inherent operating stability characteristics of the design. This includes a low susceptibility to cracking failure from the effects of corrosion (e.g., intergranular stress corrosion cracking (IGSCC)). This operating history totals over 950 reactor-years, including 13 plant each having over 25 years of operation, 12 other plant each with over 20 years of operation and 8 plant each over 15 years of operation.

In 1978, the United States Nuclear Regulatory Commission (USNRC) formed the second Pipe Crack Study Group. (The first Pipe Crack Study Group (PCSG) established in 1975 addressed cracking in boiling water reactors only.) One of the objectives of the second PCSG was to include a review of the potential for stress corrosion cracking in Pressurized Water Reactors (PWR's). The results of the study performed by the PCSG were presented in NUREG-0531 (Reference 2-1) entitled "Investigation and Evaluation of Stress-Corrosion Cracking in Piping of Light Water Reactor Plant." In that report the PCSG stated:

"The PCSG has determined that the potential for stress-corrosion cracking in PWR primary system piping is extremely low because the ingredients that produce IGSCC are not all present. The use of hydrazine additives and a hydrogen overpressure limit the oxygen in the coolant to very low levels. Other impurities that might cause stress-corrosion cracking, such as halides or caustic, are also rigidly controlled. Only for brief periods during reactor shutdown when the coolant is exposed to the air and during the subsequent startup are conditions even marginally capable of producing stress-corrosion cracking in the primary systems of PWRs. Operating experience in PWRs supports this determination. To date, no stress corrosion cracking has been reported in the primary piping or safe ends of any PWR."

During 1979, several instances of cracking in PWR feedwater piping led to the establishment of the third PCSG. The investigations of the PCSG reported in NUREG-0691 (Reference 2-2) further confirmed that no occurrences of IGSCC have been reported for PWR primary coolant systems.

As stated above, for the Westinghouse plant, there is no history of failure in the reactor coolant system loop. The discussion below further qualifies the PCSG's findings.

For stress corrosion cracking (SCC) to occur in piping, the following three conditions must exist simultaneously: high tensile stresses, susceptible material, and a corrosive environment. Since some residual stresses and some degree of material susceptibility exist in any stainless steel piping, the potential for stress corrosion is minimized by properly selecting a material immune to SCC as well as preventing the occurrence of a corrosive environment. The material specifications consider compatibility with the system's operating environment (both internal and

external) as well as other material in the system, applicable ASME Code rules, fracture toughness, welding, fabrication, and processing.

The elements of a water environment known to increase the susceptibility of austenitic stainless steel to stress corrosion are: oxygen, fluorides, chlorides, hydroxides, hydrogen peroxide, and reduced forms of sulfur (e.g., sulfides, sulfites, and thionates). Strict pipe cleaning standards prior to operation and careful control of water chemistry during plant operation are used to prevent the occurrence of a corrosive environment. Prior to being put into service, the piping is cleaned internally and externally. During flushes and pre-operational testing, water chemistry is controlled in accordance with written specifications. Requirements on chlorides, fluorides, conductivity, and pH are included in the acceptance criteria for the piping.

During plant operation, the reactor coolant water chemistry is monitored and maintained within very specific limits. Contaminant concentrations are kept below the thresholds known to be conducive to stress corrosion cracking with the major water chemistry control standards being included in the plant operating procedures as a condition for plant operation. For example, during normal power operation, oxygen concentration in the RCS is expected to be in the ppb range by controlling charging flow chemistry and maintaining hydrogen in the reactor coolant at specified concentrations. Maintaining concentrations of chlorides and fluorides within the specified limits also stringently controls halogen concentrations. Thus during plant operation, the likelihood of stress corrosion cracking is minimized.

2.2 WATER HAMMER

Overall, there is a low potential for water hammer in the RCS since it is designed and operated to preclude the voiding condition in normally filled lines. The reactor coolant system, including piping and primary components, is designed for normal, upset, emergency, and faulted condition transients. The design requirements are conservative relative to both the number of transients and their severity. Relief valve actuation and the associated hydraulic transients following valve opening are considered in the system design. Other valve and pump actuation is relatively slow transients with no significant effect on the system dynamic loads. To ensure dynamic system stability, reactor coolant parameters are stringently controlled. Temperature during normal operation is maintained within a narrow range by control rod position; pressurizer heaters and pressurizer spray also within a narrow range for steady-state conditions control pressure. The flow characteristics of the system remain constant during a fuel cycle because the only governing parameters, namely system resistance and the reactor coolant pump characteristics, are controlled in the design process. Additionally, Westinghouse has instrumented typical reactor coolant systems to verify the flow and vibration characteristics of the system. Pre-operational testing and operating experience have verified the Westinghouse approach. The operating transients of the RCS primary piping are such that no significant water hammer can occur.

2.3 LOW CYCLE AND HIGH CYCLE FATIGUE

An assessment of the low cycle fatigue loadings was carried out as part of this study in the form of a fatigue crack growth analysis, as discussed in Section 8.0.

High cycle fatigue loads in the system would result primarily from pump vibrations. These are minimized by restrictions placed on shaft vibrations during hot functional testing and operation. During operation, an alarm signals the exceedence of the vibration limits. Field measurements have been made on a number of plant during hot functional testing, including plant similar to H. B. Robinson Unit 2. Stresses in the elbow below the reactor coolant pump resulting from system vibration have been found to be very small, between 2 and 3 ksi at the highest. These stresses are well below the fatigue endurance limit for the material and would also result in an applied stress intensity factor below the threshold for fatigue crack growth.

2.4 REFERENCES

- 2-1 Investigation and Evaluation of Stress-Corrosion Cracking in Piping of Light Water Reactor Plant, NUREG-0531, U.S. Nuclear Regulatory Commission, February 1979.
- 2-2 Investigation and Evaluation of Cracking Incidents in Piping in Pressurized Water Reactors, NUREG-0691, U.S. Nuclear Regulatory Commission, September 1980.

3.0 PIPE GEOMETRY AND LOADING

3.1 INTRODUCTION TO METHODOLOGY

The general approach is discussed first. As an example, a segment of the primary coolant hot leg pipe is shown in Figure 3-1. The as-built outside diameter and minimum wall thickness of the pipe are 34.00 in. and 2.40 in., respectively, as shown in the figure. The normal stresses at the weld locations are from the load combination procedure discussed in Section 3.3 whereas the faulted loads are as described in Section 3.4. The components for normal loads are pressure, dead weight and thermal expansion. An additional component, Safe Shutdown Earthquake (SSE) is considered for faulted loads. Tables 3-1 and 3-2 show the enveloping loads for H. B. Robinson Unit 2. As seen from Table 3-2, the highest stressed location in the entire loop is at Location 1 at the reactor vessel outlet nozzle to pipe weld. This is one of the locations at which, as an enveloping location, leak-before-break is to be established. Location 1 is also the critical location for the stainless steel and Alloy 182 welds. Essentially a circumferential flaw is postulated to exist at this location which is subjected to both the normal loads and faulted loads to assess leakage and stability, respectively. The loads (developed below) at this location are also given in Figure 3-1.

Since the elbows are made of different materials locations other than highest stressed pipe location were examined taking into consideration both fracture toughness and stress. The four most critical locations are identified after the full analysis is completed. Once loads (this section) and fracture toughnesses (Section 4.0) are obtained, the critical locations are determined (Section 5.0). At these locations, leak rate evaluations (Section 6.0) and fracture mechanics evaluations (Section 7.0) are performed per the guidance of Reference 3-1. Fatigue crack growth (Section 8.0) assessment and stability margins are also evaluated (Section 9.0).

All the weld locations for evaluation are those shown in Figure 3-2.

3.2 CALCULATION OF LOADS AND STRESSES

The stresses due to axial loads and bending moments are calculated by the following equation:

$$\sigma = (F/A) + (M/Z') \quad (3-1)$$

where,

σ	=	stress
F	=	axial load
M	=	moment
A	=	pipe cross-sectional area
Z'	=	section modulus

The bending moments for the desired loading combinations are calculated by the following equation:

$$M = (M_x^2 + M_y^2 + M_z^2)^{0.5} \quad (3-2)$$

where,

- M = moment for required loading
- M_x = x component of bending moment
- M_y = y component of bending moment
- M_z = z component of bending moment

The axial load and bending moments for leak rate predictions and crack stability analyses are computed by the methods to be explained in Sections 3.3 and 3.4.

3.3 LOADS FOR LEAK RATE EVALUATION

The normal operating loads for leak rate predictions are calculated by the following equations:

$$F = F_{DW} + F_{TH} + F_P \quad (3-3)$$

$$M_x = (M_x)_{DW} + (M_x)_{TH} + (M_x)_P \quad (3-4)$$

$$M_y = (M_y)_{DW} + (M_y)_{TH} + (M_y)_P \quad (3-5)$$

$$M_z = (M_z)_{DW} + (M_z)_{TH} + (M_z)_P \quad (3-6)$$

The subscripts of the above equations represent the following loading cases:

- DW = deadweight
- TH = normal thermal expansion
- P = load due to internal pressure

This method of combining loads is often referred as the algebraic sum method (Reference 3-1).

The loads based on this method of combination are provided in Table 3-1 at all the locations identified in Figure 3-2. The as-built dimensions are also given.

3.4 LOAD COMBINATION FOR CRACK STABILITY ANALYSES

In accordance with Standard Review Plan 3.6.3 (Reference 3-1), the absolute sum of loading components can be applied which results in higher magnitude of combined loads. If crack stability is demonstrated using these loads, the LBB margin on loads can be reduced from $\sqrt{2}$ to 1.0. The absolute summation of loads are shown in the following equations:

$$F = |F_{DW}| + |F_{TH}| + |F_P| + |F_{SSEINERTIA}| + |F_{SSEAM}| \quad (3-6)$$

$$M_x = |(M_x)_{DW}| + |(M_x)_{TH}| + |(M_x)_P| + |(M_x)_{SSEINERTIA}| + |(M_x)_{SSEAM}| \quad (3-7)$$

$$M_y = |(M_y)_{DW}| + |(M_y)_{TH}| + |(M_y)_P| + |(M_y)_{SSEINERTIA}| + |(M_y)_{SSEAM}| \quad (3-8)$$

$$M_z = |(M_z)_{DW}| + |(M_z)_{TH}| + |(M_z)_P| + |(M_z)_{SSEINERTIA}| + |(M_z)_{SSEAM}| \quad (3-9)$$

where subscripts SSE, INERTIA and AM mean safe shutdown earthquake, inertia and anchor motion, respectively.

The loads so determined are used in the fracture mechanics evaluations (Section 7.0) to demonstrate the LBB margins at the locations established to be the governing locations. These loads at all the locations of interest (see Figure 3-2) are given in Table 3-2.

3.5 REFERENCES

- 3-1 Standard Review Plan: Public Comments Solicited; 3.6.3 Leak-Before-Break Evaluation Procedures; Federal Register/Vol. 52, No. 167/Friday, August 28, 1987/Notices, pp. 32626-32633.

Table 3-1 Dimensions, Normal Loads and Normal Stresses for H. B. Robinson Unit 2

Location^a	Outside Diameter (in)	Minimum Thickness (in)	Axial Load^b (kips)	Moment (in-kips)	Total Stress (ksi)
1	34.00	2.400	1492	22386	18.99
2	34.00	2.400	1492	4327	8.72
3	34.00	2.400	1492	9062	11.41
4	37.75	3.275	1849	16204	10.97
5	37.62	3.210	1665	4563	6.46
6	36.32	2.560	1654	4273	8.09
7	36.32	2.560	1651	4351	8.11
8	36.32	2.560	1706	1084	6.79
9	36.32	2.560	1706	2779	7.58
10	37.62	3.210	1801	7465	7.90
11	32.26	2.280	1354	7526	11.31
12	32.26	2.280	1354	4968	9.61
13	32.26	2.280	1354	5841	10.19
14	33.60	2.950	1339	7260	8.34

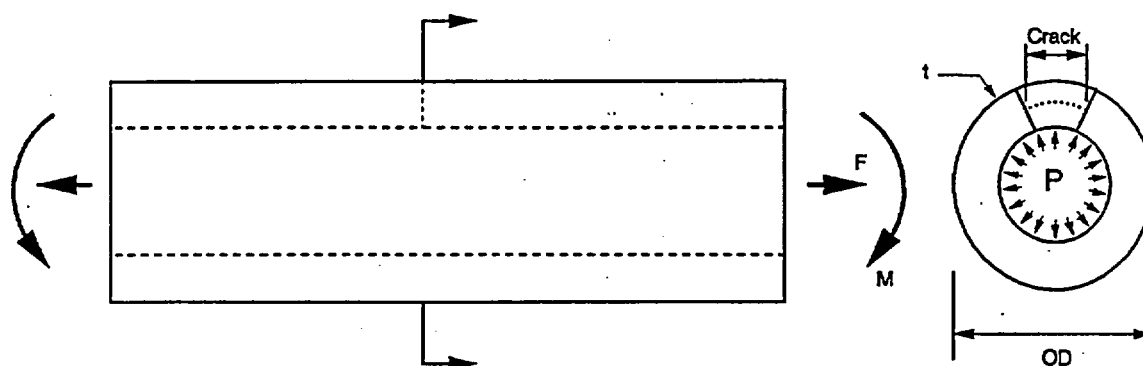
a. See Figure 3-2

b. Includes Pressure

Table 3-2 Faulted Loads and Stresses for H. B. Robinson Unit 2

Location^{a,b}	Axial Load^c (kips)	Moment (in-kips)	Total Stress (ksi)
1	1639	22824	19.85
2	1638	5076	9.76
3	1638	9714	12.40
4	1956	18794	12.19
5	1882	14302	10.62
6	1840	9572	11.25
7	1837	6079	9.60
8	1841	6355	9.75
9	1839	7233	10.15
10	1846	15456	10.93
11	1405	13288	15.38
12	1405	10660	13.63
13	1406	9465	12.84
14	1401	11305	10.57

- a. See Figure 3-2
b. See Table 3-1 for dimensions
c. Includes Pressure



$$\begin{aligned} OD^a &= 34.00 \text{ in} \\ t^a &= 2.40 \text{ in} \end{aligned}$$

Normal Loads^a

force^c: 1492 kips
moment: 22386 in-kips

Faulted Loads^b

force^c: 1639 kips
moment: 22824 in-kips

^a See Table 3-1

^b See Table 3-3

^c Includes the force due to a pressure of 2250 psia

Figure 3-1 Hot Leg Coolant Pipe

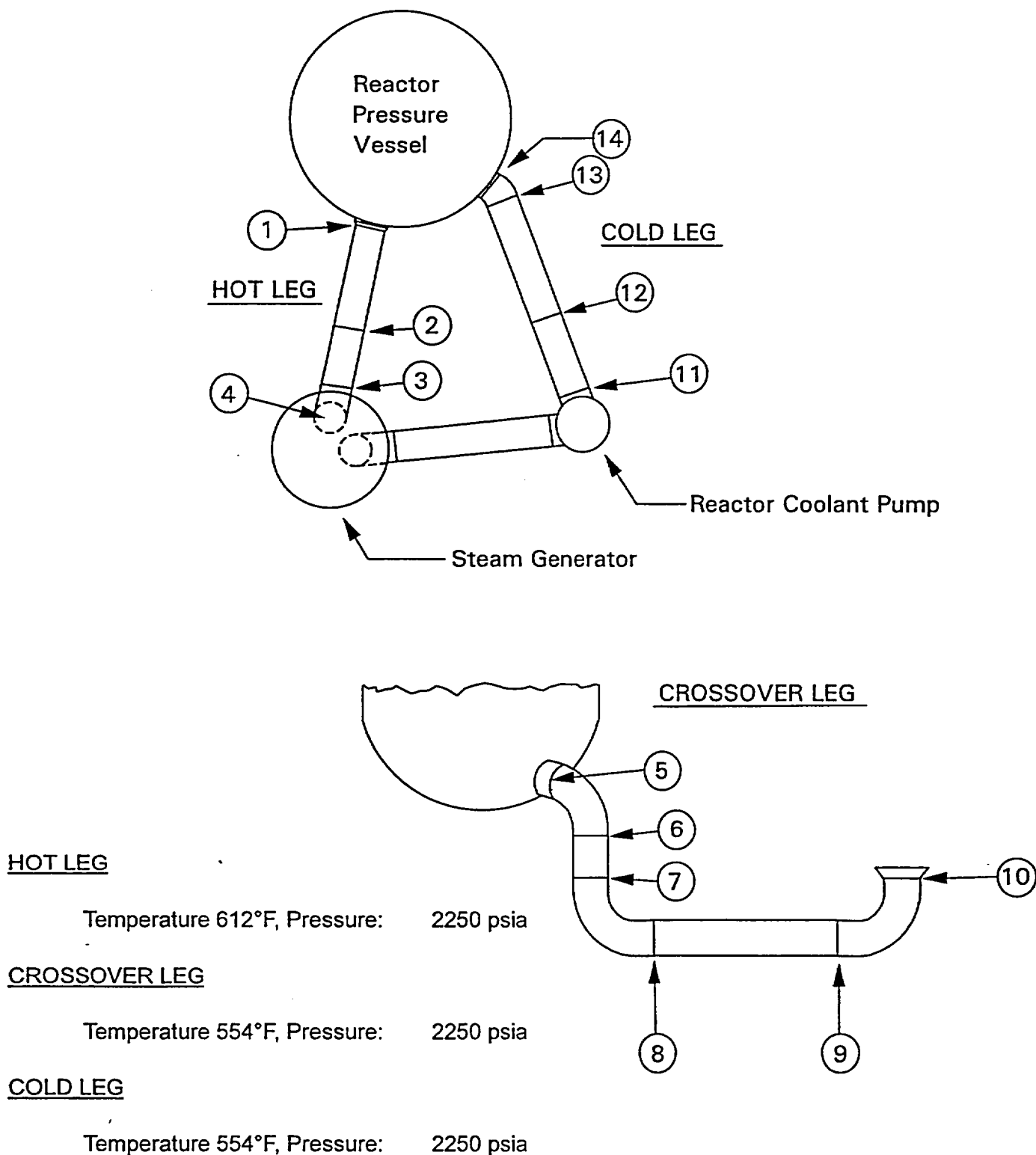


**Figure 3-2 Schematic Diagram of H. B. Robinson Unit 2
Primary Loop Showing Weld Locations**

4.0 MATERIAL CHARACTERIZATION

4.1 PRIMARY LOOP PIPE AND FITTINGS MATERIALS

The primary loop pipe is A376 TP316 and the elbow fittings are A351 CF8M for the H. B. Robinson Unit 2. Field weld process type used in the analysis is assumed as GTAW and SMAW combination and for the shop weld process type is GTAW, SMAW and SAW combination.

4.2 TENSILE PROPERTIES

The Pipe Certified Materials Test Reports (CMTRs) for H. B. Robinson Unit 2 were used to establish the tensile properties for the leak-before-break analyses. The CMTRs include tensile properties at room temperature and/or at 650°F for each of the heats of material. These properties are given in Table 4-1 for the H. B. Robinson Unit 2 pipes, Table 4-2 for the H. B. Robinson Unit 2 elbows.

The representative properties at 612°F for the pipe were established from the tensile properties at 650°F given in Table 4-1 by utilizing Section III of the 1989 ASME Boiler and Pressure Vessel Code (Reference 4-1). Code tensile properties at 612°F was obtained by interpolating between the 600°F and 650°F tensile properties. Ratios of the code tensile properties at 612°F to the corresponding tensile properties at 650°F were then applied to the 650°F tensile properties given in Table 4-1 to obtain the plant specific properties for the forged material A376 TP316 at 612°F.

The representative properties at 612°F and 554°F for the elbows were established from the tensile properties at room temperature properties given in Table 4-2 by utilizing Section III of the 1989 ASME Boiler and Pressure Vessel Code (Reference 4-1). Code tensile properties at 612°F and 554°F were obtained by interpolating between the 500°F, 600°F and 650°F tensile properties. Ratios of the code tensile properties at 612°F and 554°F to the corresponding tensile properties at room temperature were then applied to the room temperature tensile properties given in Table 4-2 to obtain the plant specific properties for the cast material A351 CF8M at 612°F and 554°F.

The average and lower bound yield strengths and ultimate strengths are given in Table 4-3. The ASME Code moduli of elasticity values are also given, and Poisson's ratio was taken as 0.3.

For leak-before-break fracture evaluations at the critical locations the true stress-true strain curves for A351 CF8M at 612°F and 554°F must be available. These curves were obtained using the Nuclear Systems Materials Handbook (Reference 4-2). The lower bound true stress-true strain curves are given in Figures 4-1 and 4-2.

4.3 FRACTURE TOUGHNESS PROPERTIES

Forged stainless steel piping such as A376 TP316 does not degrade due to thermal aging. Thus fracture toughness values well in excess of that established in the following paragraphs for the cast material and welds exist for the material throughout service life and therefore, forged material is not limiting.

The pre-service fracture toughnesses of cast stainless steels in terms of J_{Ic} have been found to be very high at 600°F. Typical results for a cast material are given in Figure 4-3. J_{Ic} is observed to be over 2500 in-lbs/in². However, cast stainless steel is susceptible to thermal aging at the reactor operating temperature, that is, about 290°C (550°F). Thermal aging of cast stainless steel results in embrittlement, that is, a decrease in the ductility, impacts strength, and fractures toughness, of the material. Depending on the material composition, the Charpy impact energy of a cast stainless steel component could decrease to a small fraction of its original value after exposure to reactor temperatures during service.

The susceptibility of the material to thermal aging increases with increasing ferrite contents. The molybdenum bearing CF8M shows increased susceptibility to thermal aging.

In 1994, the Argonne National Laboratory (ANL) completed an extensive research program in assessing the extent of thermal aging of cast stainless steel materials. The ANL research program measured mechanical properties of cast stainless steel materials after they have been heated in controlled ovens for long periods of time. ANL compiled a data base, both from data within ANL and from international sources, of about 85 compositions of cast stainless steel exposed to a temperature range of 290-400°C (550-750°F) for up to 58,000 hours (6.5 years). From this database, ANL developed correlations for estimating the extent of thermal aging of cast stainless steel (References 4-3 and 4-4).

ANL developed the fracture toughness estimation procedures by correlating data in the database conservatively. After developing the correlations, ANL validated the estimation procedures by comparing the estimated fracture toughness with the measured value for several cast stainless steel plant components removed from actual plant service. The ANL procedures produced conservative estimates that were about 30 to 50 percent less than actual measured values. The procedure developed by ANL in Reference 4-4 was used to calculate the fracture toughness values for this analysis. ANL research program was sponsored and the procedure was accepted (Reference 4-5) by the NRC.

[

J_{Ic}

[

]ace

[

 $J^{a,c,e}$

The results from the ANL Research Program indicate that the lower-bound fracture toughness of thermally aged cast stainless steel is similar to that of submerged arc welds (SAWs). The applied value of the J-integral for a flaw in the weld regions will be lower than that in the base metal because the yield stress for the weld materials is much higher at the temperature^a. Therefore, weld regions are less limiting than the cast material.

In fracture mechanics analyses that follow, the fracture toughness properties given in Table 4-5 will be used as the criteria against which the applied fracture toughness values will be compared.

4.4 REFERENCES

- 4-1 ASME Boiler and Pressure Vessel Code Section III, "Rules for construction of Nuclear Power plant Components," Appendices, July 1, 1989.
- 4-2 Nuclear Systems Materials Handbook, Part 1 – Structural Materials, Group 1 – High Alloy Steels, Section 2, ERDA Report TID 26666, November, 1975.
- 4-3 O. K. Chopra and W. J. Shack, "Assessment of Thermal Embrittlement of Cast Stainless Steels," NUREG/CR-6177, U. S. Nuclear Regulatory Commission, Washington, DC, May 1994.
- 4-4 O. K. Chopra, "Estimation of Fracture Toughness of Cast Stainless Steels During Thermal Aging in LWR Systems," NUREG-CR-4513, Revision 1, U. S. Nuclear Regulatory Commission, Washington, DC, August 1994.

^a In the report all the applied J values were conservatively determined by using base metal strength properties.

REFERENCES (Cont'd)

- 4-5 "Flaw Evaluation of Thermally aged Cast Stainless Steel in Light-Water Reactor Applications," Lee, S.; Kuo, P. T.; Wichman, K.; Chopra, O.; Published in International Journal of Pressure Vessel and Piping, June 1997.

Table 4-1 Measured Tensile Properties (psi) for H. B. Robinson Unit 2					
HEAT NO.	LOCATION	At Room Temperature		At 650°F	
		YIELD STRENGTH	ULTIMATE STRENGTH	YIELD STRENGTH	ULTIMATE STRENGTH
FO190	Hot Leg	42000	88800	21300	58200
FO190	Hot Leg	43000	86000	N/A	N/A
V0126	Hot Leg	40500	83000	23400	65200
V0126	Hot Leg	46100	90200	N/A	N/A
D8774	Hot Leg	36000	79200	24000	67400
D8774	Hot Leg	37000	79700	N/A	N/A
52152	Hot Leg	37100	77400	20800	61400
52152	Hot Leg	36500	78600	N/A	N/A
F0214	Hot Leg	42500	82300	22400	62300
F0214	Hot Leg	44500	77300	N/A	N/A
D8777	X-Over Leg	36100	78200	20800	63700
D8777	X-Over Leg	38500	77800	N/A	N/A
D8915	X-Over Leg	38500	77400	24200	62300
D8915	X-Over Leg	38600	77200	N/A	N/A
D8785	X-Over Leg	36100	74200	20400	57200
D8785	X-Over Leg	39700	79800	N/A	N/A
FO189	X-Over Leg	37700	80600	25200	70000
FO189	X-Over Leg	44100	91000	N/A	N/A
D8775	X-Over Leg	36100	77800	20500	64100
D8775	X-Over Leg	39300	79000	N/A	N/A
D8915	X-Over Leg	37700	79600	22800	62400
D8915	X-Over Leg	39300	80200	N/A	N/A
FO216	Cold Leg	40900	83000	21300	66600
FO216	Cold Leg	42500	83500	N/A	N/A
52263	Cold Leg	34200	75100	23100	63700
52263	Cold Leg	37800	75200	N/A	N/A
D8768	Cold Leg	36000	83000	23800	71700
D8768	Cold Leg	39300	82700	N/A	N/A
52152	Cold Leg	44400	89700	21600	58800
52152	Cold Leg	34899	75200	N/A	N/A
V0342	Cold Leg	35100	75200	25600	52500
V0342	Cold Leg	36100	75100	N/A	N/A
D8913	Cold Leg	35100	78400	24300	68500
D8913	Cold Leg	41100	84800	N/A	N/A

**Table 4-2 Measured Tensile Properties (psi) for H. B. Robinson
Unit 2 Primary Loop Elbows**

HEAT NO.	LOCATION	At Room Temperature	
		YIELD STRENGTH	ULTIMATE STRENGTH
4204	Hot Leg	43500	87500
7896	Hot Leg	43500	87500
8066	Hot Leg	49500	88500
3327	X-over Leg	51000	90000
6079	X-over Leg	54000	93800
6185	X-over Leg	43500	87500
9390A	X-over Leg	45000	88500
9517	X-over Leg	48000	89000
9436	X-over Leg	45000	88500
9476	X-over Leg	43500	85500
9964	X-over Leg	48000	90000
10165	X-over Leg	55500	96500
9305A	X-over Leg	51000	91500
9640	X-over Leg	48000	88000
9720	X-over Leg	45750	88000
9760	X-over Leg	45500	89500
9841	X-over Leg	45000	88500
9882	X-over Leg	45000	85500
4589	Cold Leg	45000	89000
5065	Cold Leg	45000	87500
5529	Cold Leg	54000	96000

Table 4-3 Mechanical Properties for H. B. Robinson Unit 2 Materials at Operating Temperatures

Material	Temperature (°F)	Average Yield Strength (psi)	Lower Bound	
			Yield Stress (psi)	Ultimate Strength (psi)
A376 TP316	612	22,955	20,651	52,500
A351 CF8M	612	29,556	27,156	81,836
	554	30,468	27,994	81,836
Modulus of Elasticity				
E = 25.24x 10 ⁶ psi, at 612°F				
E = 25.53 x 10 ⁶ psi, at 554°F				
Poisson's ratio: 0.3				

a,c,e

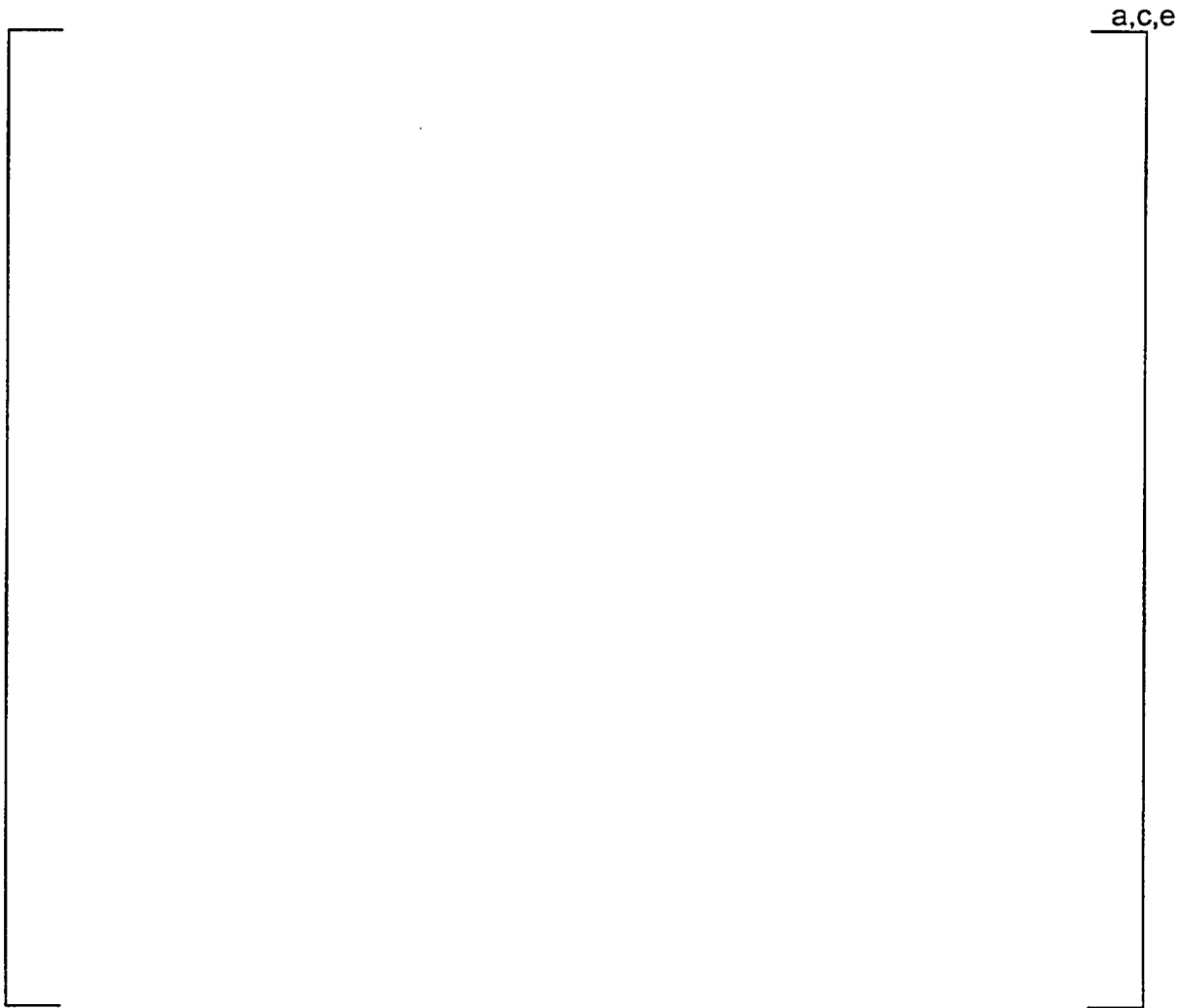


Figure 4-1 Representative Lower Bound True Stress - True Strain Curve for A351 CF8M at 612°F

a,c,e

**Figure 4-2 Representative Lower Bound True Stress - True Strain Curve for
A351 CF8M at 554°F**

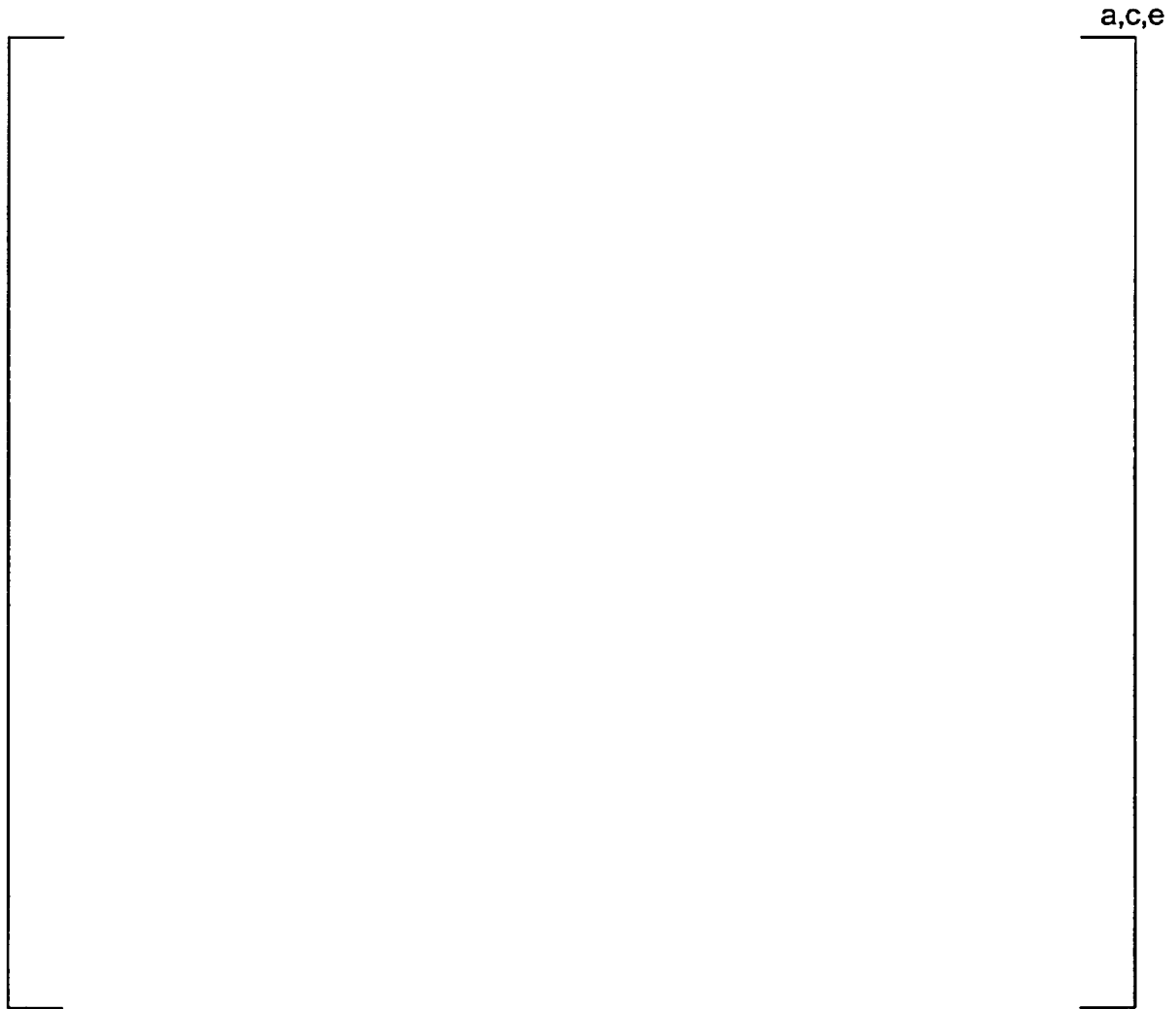


Figure 4-3 Pre-Service J vs. Δa for SA351 CF8M Cast Stainless Steel at 600°F

5.0 CRITICAL LOCATIONS AND EVALUATION CRITERIA

5.1 CRITICAL LOCATIONS

The leak-before-break (LBB) evaluation margins are to be demonstrated for the limiting locations (governing locations). Such locations are established based on the loads (Section 3.0) and the material properties established in Section 4.0. These locations are defined below for H. B. Robinson Unit 2. Table 3-2 as well as Figure 3-2 is used for this evaluation.

Critical Locations

The highest stressed location for the entire primary loop is at Location 1 (in the Hot Leg) (See Figure 3-2) at the reactor vessel outlet nozzle to pipe weld. Location 1 is the critical weld location for pipe. Location 1 is also the critical location for the stainless steel and Alloy 182 welds.

Since the elbows are made of cast materials, the critical weld locations for the elbows are as follows. For the hot leg the highest stressed location is at weld location 3, for the cross-over leg the highest stressed location is at weld location 6 and for the cold leg the highest stressed location is at weld location 13. It is thus concluded that the enveloping locations in H. B. Robinson Unit 2 for which LBB methodology is to be applied are locations 1, 3, 6 and 13. The tensile properties and the allowable toughness for the critical locations are shown in Tables 4-3 and 4-5.

5.2 FRACTURE CRITERIA

As will be discussed later, fracture mechanics analyses are made based on loads and postulated flaw sizes related to leakage. The stability criteria against which the calculated J and tearing modulus are compared are:

- (1) If $J_{app} < J_{IC}$, then the crack will not initiate;
- (2) If $J_{app} \geq J_{IC}$, but, if $T_{app} < T_{mat}$ and $J_{app} < J_{max}$, then the crack is stable.

Where: J_{app} = Applied J

J_{IC} = J at Crack Initiation

T_{app} = Applied Tearing Modulus

T_{mat} = Material Tearing Modulus

J_{max} = Maximum J value of the material

For critical locations, the limit load method discussed in Section 7.0 was also used.

6.0 LEAK RATE PREDICTIONS

6.1 INTRODUCTION

The purpose of this section is to discuss the method, which is used to predict the flow through postulated through-wall cracks and present the leak rate calculation results for through-wall circumferential cracks.

6.2 GENERAL CONSIDERATIONS

The flow of hot pressurized water through an opening to a lower back pressure causes flashing, which can result in choking. For long channels where the ratio of the channel length, L , to hydraulic diameter, D_H , (L/D_H) is greater than [

$$]^{a,c,e}.$$

6.3 CALCULATION METHOD

The basic method used in the leak rate calculations is the method developed by [

$$]^{a,c,e}$$

The flow rate through a crack was calculated in the following manner. Figure 6-1 from Reference 6-1 was used to estimate the critical pressure, P_c , for the primary loop enthalpy condition and an assumed flow. Once P_c was found for a given mass flow, the [

$]^{a,c,e}$ was found from Figure 6-2 (taken from

Reference 6-1). For all cases considered, since [$]^{a,c,e}$.

Therefore, this method will yield the two-phase pressure drop due to momentum effects as illustrated in Figure 6-3, where P_o is the operating pressure. Now using the assumed flow rate, G , the frictional pressure drop can be calculated using

$$\Delta P_f = [\quad]^{a,c,e} \quad (6-1)$$

where the friction factor f is determined using the [$]^{a,c,e}$ The crack relative roughness, ϵ , was obtained from fatigue crack data on stainless steel samples. The relative roughness value used in these calculations was [$]^{a,c,e}$

The frictional pressure drop using equation 6-1 is then calculated for the assumed flow rate and added to the [$]^{a,c,e}$ to obtain the total pressure drop from the primary system to the atmosphere. That is, for the primary loop

$$\text{Absolute Pressure} - 14.7 = [\quad]^{a,c,e} \quad (6-2)$$

for a given assumed flow rate G. If the right-hand side of equation 6-2 does not agree with the pressure difference between the primary loop and the atmosphere, then the procedure is repeated until equation 6-2 is satisfied to within an acceptable tolerance which in turn leads to correct flow rate value for a given crack size.

6.4 LEAK RATE CALCULATIONS

Leak rate calculations were made as a function of crack length at the governing locations previously identified in Section 5.1. The normal operating loads of Table 3-1 was applied, in these calculations. The crack opening areas were estimated using the method of Reference 6-2 and the leak rates were calculated using the two-phase flow formulation described above. The average material properties of Section 4.0 (see Table 4-3) were used for these calculations.

The flaw sizes to yield a leak rate of 10 gpm were calculated at the governing locations and are given in Table 6-1. The flaw sizes so determined are called leakage flaw sizes.

The H. B. Robinson Unit 2 RCS pressure boundary leak detection system meets the intent of Reg. Guide 1.45, which is 1 gpm in 1 hour or less. Thus, to satisfy the margin of 10 on the leak rate, the flaw sizes (leakage flaw sizes) are determined which yield a leak rate of 10 gpm.

6.5 REFERENCES

6-1 [

]^{a,c,e}.

6-2 Tada, H., "The Effects of Shell Corrections on Stress Intensity Factors and the Crack Opening Area of Circumferential and a Longitudinal Through-Crack in a Pipe," Section II-1, NUREG/CR-3464, September 1983.

Table 6-1 Flaw Sizes Yielding a Leak Rate of 10 gpm at the Governing Locations	
Location	Leakage Flaw Size (in)
1 *	3.64
3	6.06
6	7.42
13	5.94

* [

] a,c,e



Figure 6-1 Analytical Predictions of Critical Flow Rates of Steam-Water Mixtures

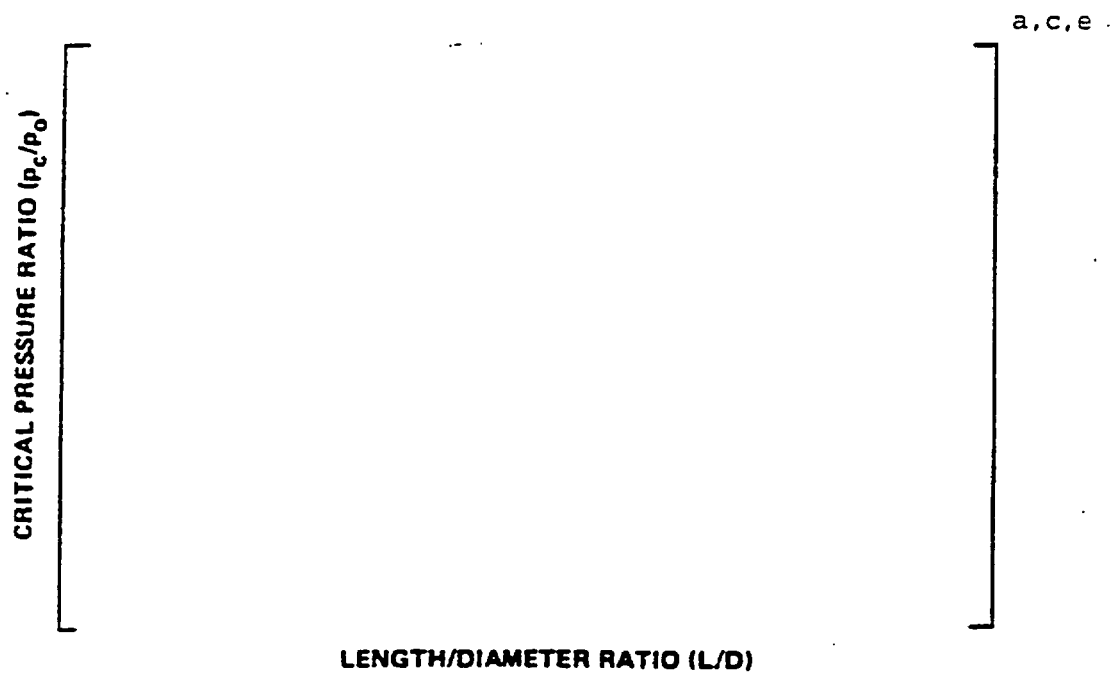


Figure 6-2 [

] ^{a,c,e} Pressure Ratio as a Function of L/D

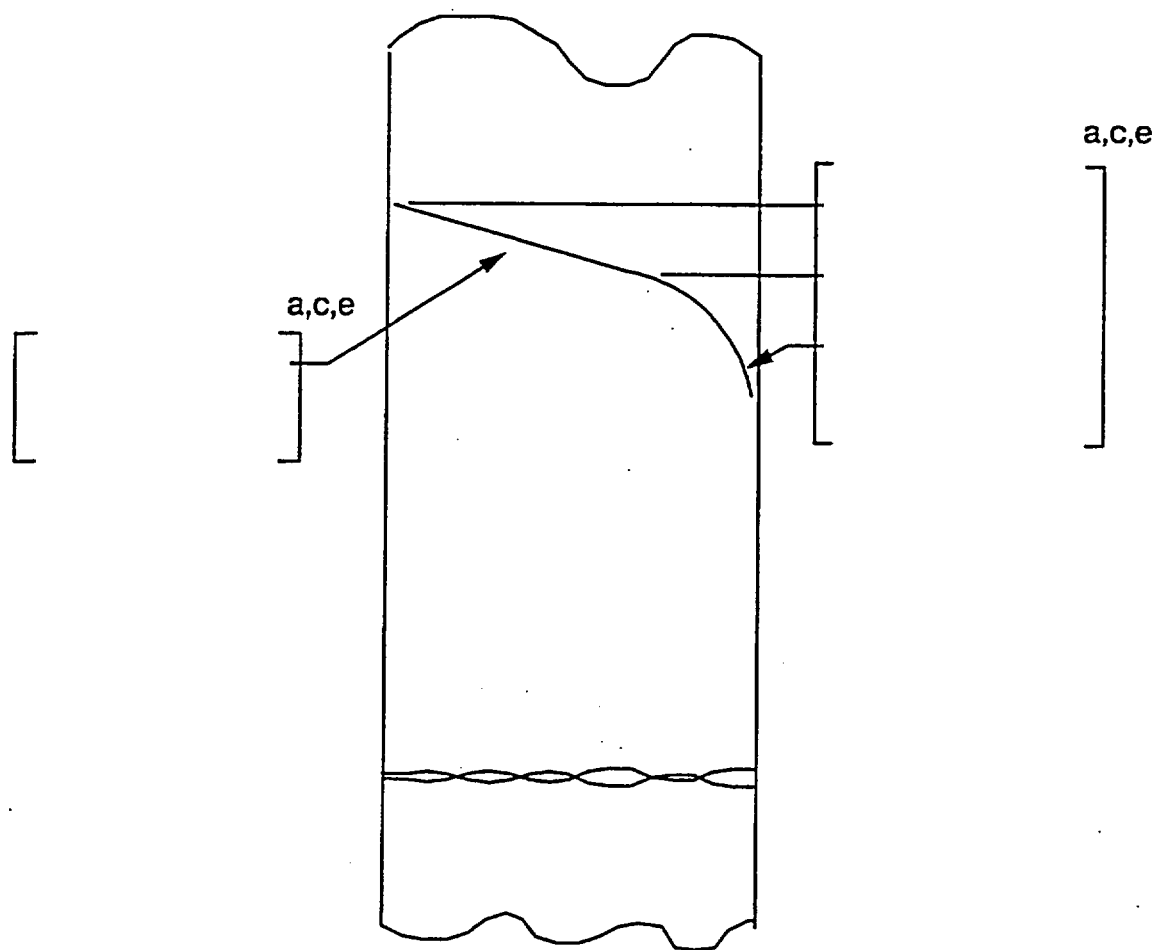


Figure 6-3 Idealized Pressure Drop Profile Through a Postulated Crack

7.0 FRACTURE MECHANICS EVALUATION

7.1 LOCAL FAILURE MECHANISM

The local mechanism of failure is primarily dominated by the crack tip behavior in terms of crack-tip blunting, initiation, extension and finally crack instability. The local stability will be assumed if the crack does not initiate at all. It has been accepted that the initiation toughness measured in terms of J_{Ic} from a J-integral resistance curve is a material parameter defining the crack initiation. If, for a given load, the calculated J-integral value is shown to be less than the J_{Ic} of the material, then the crack will not initiate. If the initiation criterion is not met, one can calculate the tearing modulus as defined by the following relation:

$$T_{app} = \frac{dJ}{da} \frac{E}{\sigma_f^2}$$

where:

T_{app}	=	applied tearing modulus
E	=	modulus of elasticity
σ_f	=	$0.5 (\sigma_y + \sigma_u)$ (flow stress)
a	=	crack length
σ_y, σ_u	=	yield and ultimate strength of the material, respectively

Stability is said to exist when ductile tearing occurs if T_{app} is less than T_{mat} , the experimentally determined tearing modulus. Since a constant T_{mat} is assumed a further restriction is placed in J_{app} . J_{app} must be less than J_{max} where J_{max} is the maximum value of J for which the experimental T is greater than or equal to the T_{mat} used.

As discussed in Section 5.2 the local crack stability criteria is a two-step process:

(1) If $J_{app} < J_{Ic}$, then the crack will not initiate.

(2) If $J_{app} > J_{Ic}$, but, if $T_{app} < T_{mat}$

and $J_{app} < J_{max}$, then the crack is stable.

7.2 GLOBAL FAILURE MECHANISM

Determination of the conditions, which lead, to failure in stainless steel should be done with plastic fracture methodology because of the large amount of deformation accompanying fracture. One method for predicting the failure of ductile material is the plastic instability

method, based on traditional plastic limit load concepts, but accounting for strain hardening and taking into account the presence of a flaw. The flawed pipe is predicted to fail when the remaining net section reaches a stress level at which a plastic hinge is formed. The stress level at which this occurs is termed as the flow stress. The flow stress is generally taken as the average of the yield and ultimate tensile strength of the material at the temperature of interest. This methodology has been shown to be applicable to ductile piping through a large number of experiments and will be used here to predict the critical flaw size in the primary coolant piping. The failure criterion has been obtained by requiring equilibrium of the section containing the flaw (Figure 7-1) when loads are applied. The detailed development is provided in appendix A for a through-wall circumferential flaw in a pipe with internal pressure, axial force, and imposed bending moments. The limit moment for such a pipe is given by:

$$[\dots]^{a,c,e}$$

where:

$$[\dots]^{a,c,e}$$

$$\sigma_f = 0.5 (\sigma_y + \sigma_u) \text{ (flow stress), psi}$$

$$[\dots]^{a,c,e}$$

$$[$$

$$]^{a,c,e}$$

The analytical model described above accurately accounts for the piping internal pressure as well as imposed axial force as they affect the limit moment. Good agreement was found between the analytical predictions and the experimental results (Reference 7-1).

For application of the limit load methodology, the material, including consideration of the configuration, must have a sufficient ductility and ductile tearing resistance to sustain the limit load.

7.3 RESULTS OF CRACK STABILITY EVALUATION

J-integral Method:

Stability analyses were performed at the critical locations established in Section 5.1. The elastic-plastic fracture mechanics (EPFM) J-integral analyses for the through-wall circumferential cracks in a cylinder were performed using the procedure in the EPRI fracture mechanics handbook (Reference 7-2). Table 7-1 shows the J-integral analysis results. As shown in this table J_{app} values are less than J_{IC} for the critical flaw size(s) of two times the 10gpm leakage flaw size(s) and therefore, stability criteria was satisfied and also margin on flaw size of 2.0 was satisfied.

Limit Load Method:

A stability analysis based on limit load was performed for all the critical locations (locations 1, 3, 6 and 13) as described in Section 7.2. The field weld at location 1 is made of GTAW and SMAW combination weld. The shop welds are assumed to be made of GTAW, SMAW or SAW combination weld. Field weld is at critical location 1. Shop welds are at critical locations 3, 6 and 13. The "Z" factor correction for GTAW is 1.0. The "Z" factor correction for SMAW was applied (Reference 7-3) at the field weld critical location (location 1) and the "Z" factor correction for SAW was applied (Reference 7-3) at the shop weld locations (locations 3, 6 and 13) and the equations are as follows:

$$Z = 1.15 [1.0 + 0.013 (OD-4)] \quad \text{For SMAW}$$

$$Z = 1.30 [1.0 + 0.01 (OD-4)] \quad \text{For SAW}$$

where OD is the outer diameter of the pipe in inches.

The Z-factors were calculated for the critical locations, using the dimensions given in Table 3-1. The Z factor was 1.599 for location 1, 1.69 for location 3, 1.72 for location 6 and 1.667 for location 13. The applied loads were increased by the Z factors and plots of limit load versus crack length were generated as shown in Figures 7-2, 7-3, 7-4 and 7-5. Table 7-2 summarizes the results of the stability analyses based on limit load. The leakage flaw sizes are also presented on the same table.

For the Alloy 182 weld critical flaw size by LIMIT load method is also shown in Table 7-2. 'Z' factor correction for the Alloy 182 weld is 1.0. As shown in Table 7-2 the margin between the critical flaw size(s) and the leakage flaw size(s) is more than 2.0 and therefore, flaw size margin criteria of 2.0 was satisfied.

7.4 REFERENCES

- 7-1 Kanninen, M. F., et. al., "Mechanical Fracture Predictions for Sensitized Stainless Steel Piping with Circumferential Cracks," EPRI NP-192, September 1976.
- 7-2 Kumar, V., German, M. D. and Shih, C. P., "An Engineering Approach for Elastic-Plastic Fracture Analysis," EPRI Report NP-1931, Project 1237-1, Electric Power Research Institute, July 1981.
- 7-3 Standard Review Plan; Public Comment Solicited; 3.6.3 Leak-Before-Break Evaluation Procedures; Federal Register/Vol. 52, No. 167/Friday, August 28, 1987/Notices, pp. 32626-32633.

a,c,e

* Not calculated since not required for the analysis results.

Note: T_{app} is not applicable since $J_{app} < J_{IC}$

Table 7-2 Stability Results for H. B. Robinson Unit 2 Based on Limit Load		
Location	Critical Flaw Size (in)	Leakage Flaw Size (in)
1*	19.70	3.64
3	38.04	6.06
6	42.07	7.42
13	36.28	5.94

* [

] a,c,e

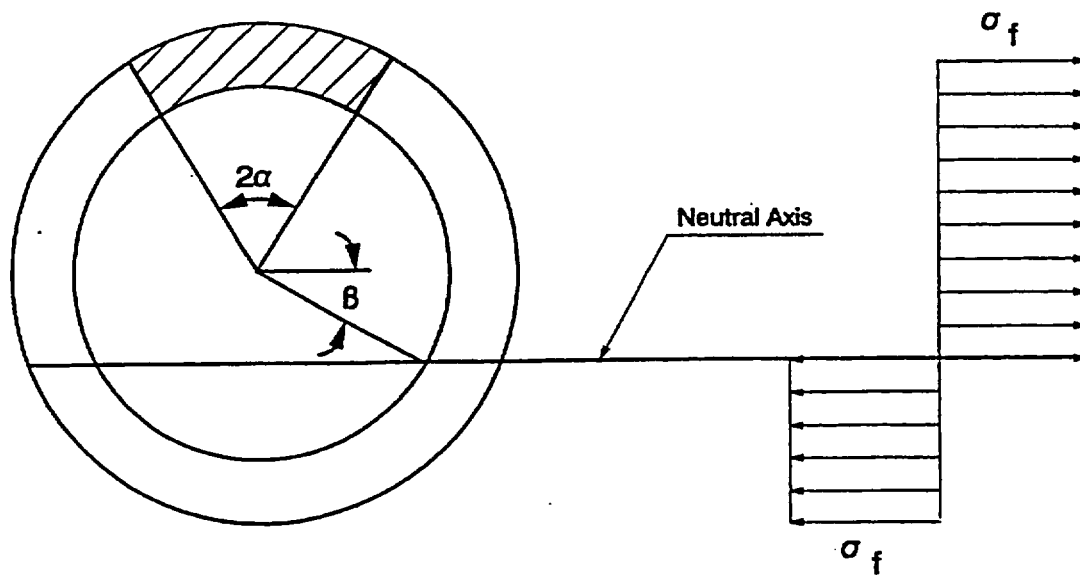


Figure 7-1 []^{a,c,e} Stress Distribution



OD = 34.00 in.

$\sigma_y = 20.65$ ksi

F = 1639 kips

t = 2.40 in.

$\sigma_u = 52.50$ ksi

M = 22824 in-kips

A376 – TP316 with SMAW weld

Figure 7-2 Critical Flaw Size Prediction - Hot Leg at Location 1



OD = 34.00 in.

$\sigma_y = 27.16$ ksi

F = 1638 kips

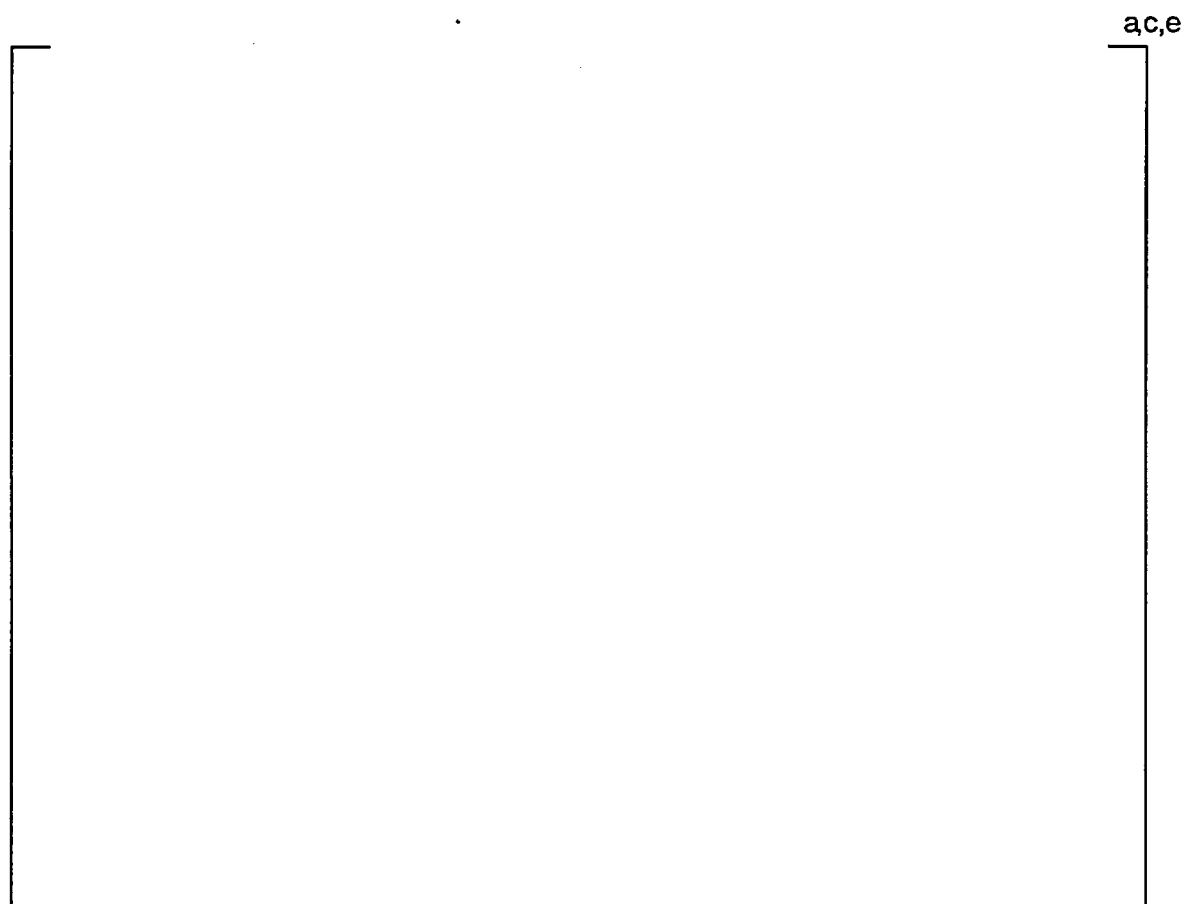
t = 2.40 in.

$\sigma_u = 81.84$ ksi

M = 9714 in-kips

A351 – CF8M with SAW weld

Figure 7-3 Critical Flaw Size Prediction – Hot Leg at Location 3



OD = 36.32 in.

$\sigma_y = 27.99$ ksi

F = 1840 kips

t = 2.56 in.

$\sigma_u = 81.84$ ksi

M = 9572 in-kips

A351 – CF8M with SAW weld

Figure 7-4 Critical Flaw Size Prediction – Cross-Over Leg at Location 6



OD = 32.26 in.

$\sigma_y = 27.99$ ksi

F = 1406 kips

t = 2.28 in.

$\sigma_u = 81.84$ ksi

M = 9465 in-kips

A351 – CF8M with SAW weld

Figure 7-5 Critical Flaw Size Prediction – Cold Leg at Location 13

8.0 FATIGUE CRACK GROWTH ANALYSIS

To determine the sensitivity of the primary coolant system to the presence of small cracks, a fatigue crack growth analysis was carried out for the Reactor vessel inlet nozzle safe-end and the outlet nozzle safe-end regions (see Locations 1 and 14 of Figure 3-2). These regions were selected because crack growth calculated in these regions would be typical of that in the entire primary loop. Crack growths calculated at other locations could be expected to show less than 10% variation.

The methods used in the fatigue crack growth analysis reported here are the same as those suggested by Section XI of the ASME Code. The analysis procedure involves postulating an initial flaw at specific regions and predicting the growth of that flaw due to an imposed series of loading transients. The input required for a fatigue crack growth analysis is basically the information necessary to calculate the parameter ΔK_I , which depends on crack and structure geometry and the range of applied stresses in the area where the crack exists. Once ΔK_I is calculated, the growth due to that particular stress cycle can be calculated. This increment of growth is then added to the original crack size, and the analysis proceeds to the next transient. The procedure is continued in this manner until all the transients predicted to occur in the period of evaluation have been analyzed.

The transients used for the fatigue crack growth of the H. B. Robinson Unit 2 plant are listed in Table 8-1. The transients used in this evaluation are not those contained in the original equipment specification (Reference 8-1); instead, the latest transient specification available has been used.

All normal, upset and test conditions were considered. A summary of applied transients is provided in Table 8-1. Circumferentially oriented surface flaws were postulated in these regions, assuming the flaw was located in three different locations, as shown in Figure 8-1. Specifically, these were:

Cross Section A: Inconel

Cross Section B: SA 508 Class 2 or 3 Low Alloy Steel

Cross Section C: Stainless Steel

CRACK GROWTH RATE REFERENCE CURVES - FERRITIC STEEL

The crack growth rate curves used in the analyses were taken directly from Appendix A of Section XI of the ASME Code. Water environment curves were used for all inside surface flaws, and the air environment curve was used for embedded flaws and outside surface flaws.

For water environments the reference crack growth curves are shown in Figure 8-2, and growth rate is a function of both the applied stress intensity factor range, and the R ratio (K_{min}/K_{max}) for the transient.

For $R \leq 0.25$

$$\left(\Delta K_I < 19 \text{ ksi} \sqrt{\text{in}} \right), \frac{da}{dN} = \left(1.02 \times 10^{-6} \right) \Delta K_I^{5.95} \quad (8-1)$$

$$\left(\Delta K_I \geq 19 \text{ ksi} \sqrt{\text{in}} \right), \left(da/dN \right) = \left(1.01 \times 10^{-1} \right) \Delta K_I^{1.95}$$

where, $\frac{da}{dN}$ = Crack Growth rate, micro-inches/cycle.

For $R \geq 0.65$

$$\left(\Delta K_I < 12 \text{ ksi} \sqrt{\text{in}} \right), \frac{da}{dN} = \left(1.20 \times 10^{-5} \right) \Delta K_I^{5.95} \quad (8-2)$$

$$\left(\Delta K_I \geq 12 \text{ ksi} \sqrt{\text{in}} \right), \left(da/dN \right) = \left(2.52 \times 10^{-1} \right) \Delta K_I^{1.95}$$

For R ratio between these two extremes, interpolation is recommended.

The crack growth rate reference curve for air environments is a single curve, with growth rate being only a function of applied ΔK . This reference curve is also shown in Figure 8-2.

$$\frac{da}{dN} = \left(0.0267 \times 10^{-3} \right) \Delta K_I^{3.726} \quad (8-3)$$

where, $\frac{da}{dN}$ = Crack growth rate, micro-inches/cycle

ΔK_I = stress intensity factor range, ksi $\sqrt{\text{in}}$

= $(K_{I\text{max}} - K_{I\text{min}})$

FATIGUE CRACK GROWTH RATE REFERENCE CURVES - STAINLESS STEEL

The reference crack growth law used for the stainless steel portions of the system was taken from that developed by the Metal Properties Council - Pressure Vessel Research Committee Task Force In Crack Propagation Technology. The reference curve has the equation:

[

$$J^{a,c,e}$$

This equation appears in Section XI, Appendix C (1989 Addendum) for air environments and its basis is provided in Reference 8-2, and shown in Figure 8-3. For water environments, an environmental factor of 2 was used, based on the crack growth tests in PWR environments reported in Reference 8-3.

FATIGUE CRACK GROWTH RATE REFERENCE CURVES - ALLOY 600, 182, AND 82 MATERIALS

The crack growth rate reference curves for these nickel base alloys have not been developed for the ASME Code, so information was obtained from the literature. The crack growth rate is a function of both R Ratio (K_{min}/K_{max}) and the range of applied stress intensity factor. Using the results reported in references 8-4 and 8-5 a curve was developed for application to a water environment, as shown below.

$$\frac{da}{dN} = 2.23 \times 10^{-13} \left[\Delta K / (1.0 - 0.5R) \right]^{5.66} \quad (8-5)$$

The crack growth rate law is slightly steeper than that for stainless steel.

RESULTS AND CONCLUSIONS

The transients and cycles for the H. B. Robinson Unit 2 plant for 60 years are the same as those of 40 years. It is therefore concluded that the fatigue crack growth analysis shown in Table 8-2 and Table 8-3 is applicable for 60 years. The results show that fatigue crack growth is not a concern for the H. B. Robinson Unit 2 primary loop piping.

As shown in Tables 8-2 and 8-3 fatigue crack growth is not significant and it is therefore expected that with a reasonable increase in transient cycles these should also be of no concern for the fatigue crack growth.

8.1 References:

- 8-1 Westinghouse Equipment Specification Number 676413 - Rev. 4, and Addendum 952542, 1973.
- 8-2 James, L. A., and Jones, D. P., "Fatigue Crack Growth Correlations for Austenitic Stainless Steel in Air," in Predictive Capabilities in Environmentally Assisted Cracking," ASME publication PVP-99, Dec. 1985..
- 8-3 Bamford, W. H., "Fatigue Crack Growth of Stainless Steel Piping in a Pressurized Water Reactor Environment," Trans ASME, Journal of Pressure Vessel Technology, Feb. 1979. Engineering Development Labs Report HEDL-TME-76-43, May 1976.
- 8-4 James, L. A., "Fatigue Crack Propagation Behavior of Inconel 600," in Hanford Engineering Labs Report HEDL-TME-76-43, May 1976.
- 8-5 Hale, D. A. et al., "Fatigue Crack Growth in Piping and RPV Steels in Simulated BWR Water Environment.

Table 8-1 Summary of Reactor Vessel Transients		
Number	Transient Identification	Number of Occurrences
	Normal Conditions	
1	Heatup and Cooldown	200
2	Unit Loading and Unloading between 15% and 100% @5% of Full Power	18300
3	Unit Loading and Unloading between 0% and 15% of Full Power	500
4	Step Load increase and decrease	2000
5	Large Step load decrease, with steam dump	200
6	Steady State Fluctuations	150000
7	Random Fluctuations	3000000
8	Feedwater Cycling	2000
9	Refueling	80
10	Loss of Load	80
11	Loss of Power	40
12	Loss of Flow	80
13	Reactor Trip with no Cooldown	230
14	Reactor Trip with Cooldown, no SI	160
15	Reactor Trip with Cooldown, and SI	10
16	Inadvertent RCS Depressurization	60
17	Inadvertent Startup of an Inactive Loop	20
18	Inadvertent SI Actuation	60
19	Control Rod Drop	80

Table 8-1 Summary of Reactor Vessel Transients (cont.)		
Number	Transient Identification	Number of Occurrences
	Test Conditions	
20	Excessive Feedwater Flow	30
21	Boron Concentration	26400
22	Loop Out-of-Service, Normal Loop Startup	70
23	Loop Out-of-Service, Normal Loop Shutdown	80
24	Primary Side Leak Test	200
25	OBE	200

Table 8-2 Fatigue Crack Growth at RPV Inlet Nozzle Safe-End Region (40 and 60 years)

	FINAL FLAW (in.)		
Initial Flaw (in.)	Ferritic Steel	Stainless	Inconel
0.305	0.3069	0.3066	0.3053
0.458	0.4644	0.4609	0.4590
0.610	0.6194	0.6141	0.6123

Table 8-3 Fatigue Crack Growth at RPV Outlet Nozzle Safe-End Region (40 and 60 years)

	FINAL FLAW (in.)		
Initial Flaw (in.)	Ferritic Steel	Stainless	Inconel
0.250	0.2761	0.2677	0.2525
0.375	0.4664	0.4119	0.3840
0.500	0.6128	0.5505	0.5160



T = Thickness
R = Inside Radius

Figure 8-1 Typical Cross-Section of RPV Inlet and Outlet Nozzle Safe-End

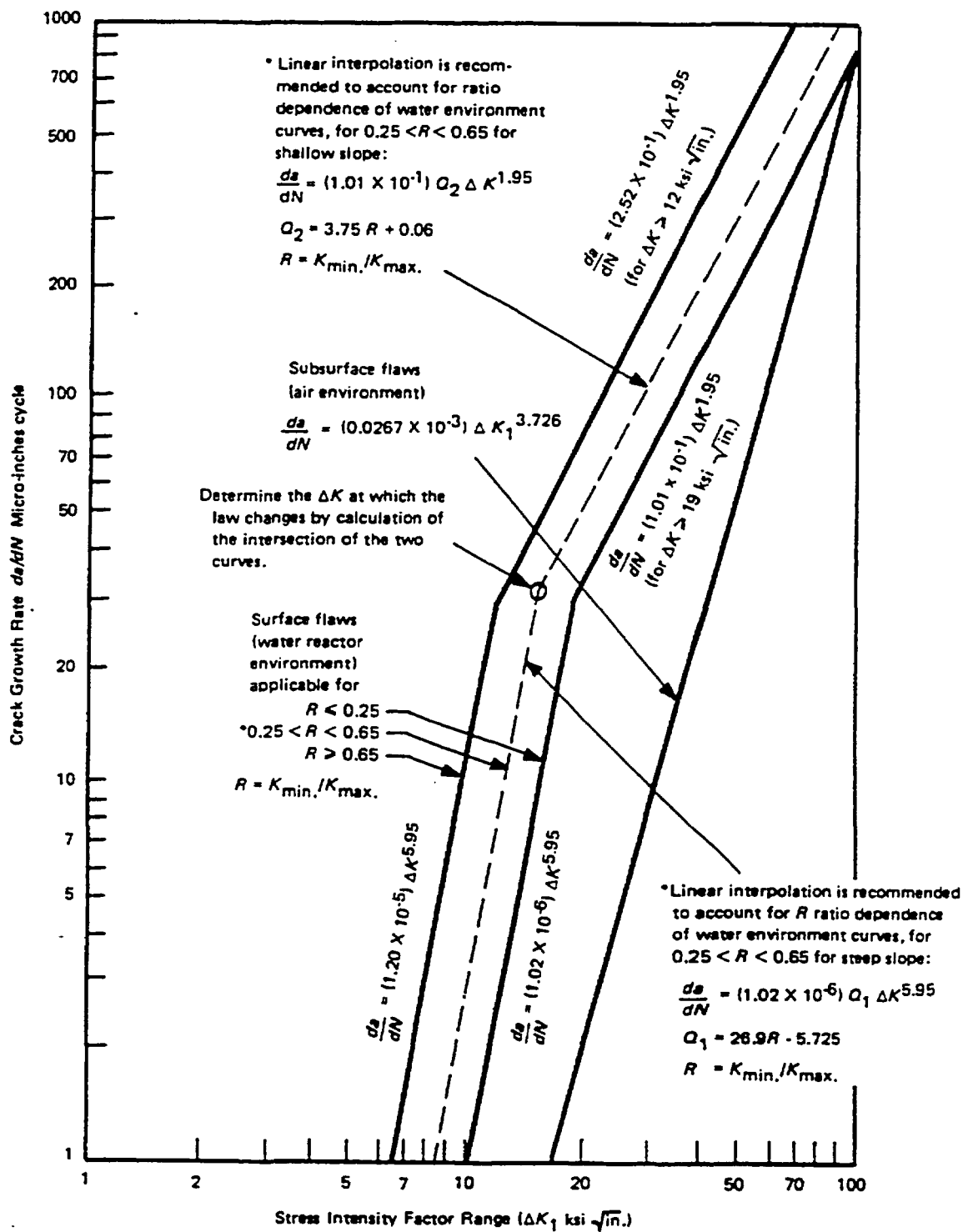


Figure 8-2 Reference Fatigue Crack Growth Curves for Carbon and Low Alloy Ferritic Steels

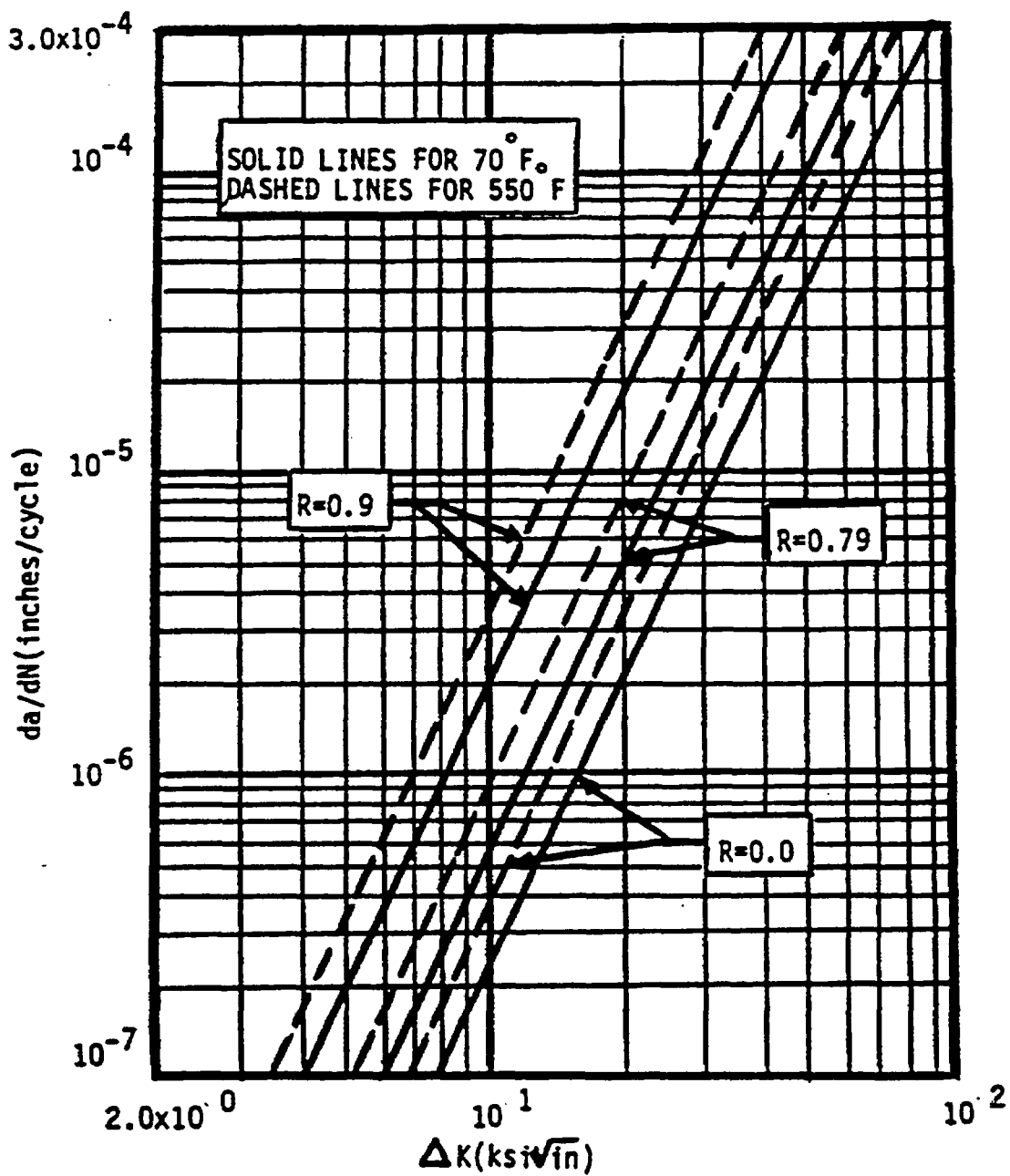
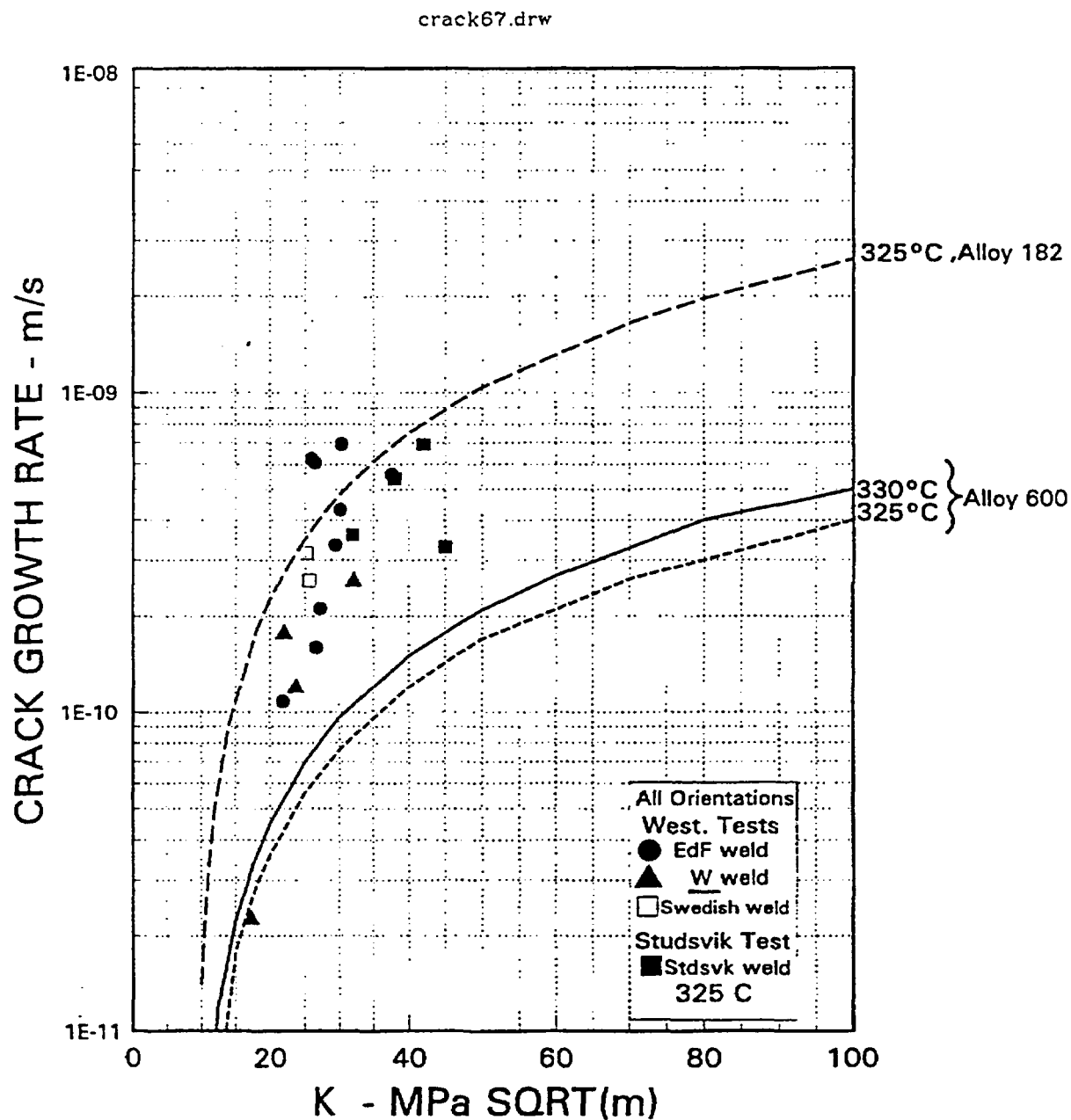


Figure 8-3 Reference Crack Growth Curves for Stainless Steel in Air Environments



SUMMARY OF WESTINGHOUSE AND STUDSVIK DATA
TYPE 182 WELDS AT 325 C

Figure 8-4 Crack Growth Model for Alloy in PWR Environments with Available Data

9.0 ASSESSMENT OF MARGINS

The results of the leak rates of Section 6.4 and the corresponding stability and fracture toughness evaluations of Sections 7.1, 7.2 and 7.3 are used in performing the assessment of margins. Margins are shown in Table 9-1.

In summary, at all the critical locations relative to:

1. Flaw Size - Using faulted loads obtained by the absolute sum method, a margin of 2 or more exists between the critical flaw and the flaw having a leak rate of 10 gpm (the leakage flaw).
2. Leak Rate - A margin of 10 exists between the calculated leak rate from the leakage flaw and the leak detection capability of 1 gpm.
3. Loads - At the critical locations the leakage flaw was shown to be stable using the faulted loads obtained by the absolute sum method (i.e., a flaw twice the leakage flaw size is shown to be stable; hence the leakage flaw size is stable). A margin of >1 on loads using the absolute summation of faulted load combinations is satisfied as per SRP 3.6.3.

**Table 9-1 Leakage Flaw Sizes, Critical Flaw Sizes and Margins for
H. B. Robinson Unit 2**

Location	Leakage Flaw Size	Critical Flaw Size	Margin
1	3.64 in.	19.70 ^a in.	5.4 ^a
3	6.06 in.	38.04 ^a in.	6.3 ^a
3	6.06 in.	12.12 ^b in.	>2.0 ^b
6	7.42 in.	42.07 ^a in.	5.7 ^a
6	7.42 in.	14.84 ^b in.	>2.0 ^b
13	5.94 in.	36.28 ^a in.	6.1 ^a
13	5.94 in.	11.88 ^b in.	>2.0 ^b

[

J^{a,c,e}

^abased on limit load

^bbased on J-integral evaluation (Note: critical flaw size postulated for the J-integral calculation is two times the leakage flaw size)

10.0 CONCLUSIONS

This report justifies the elimination of RCS primary loop pipe breaks from the structural design basis for the H. B. Robinson Unit 2 as follows:

- a. Stress corrosion cracking is precluded by use of fracture resistant materials in the piping system and controls on reactor coolant chemistry, temperature, pressure, and flow during normal operation.
- b. Water hammer should not occur in the RCS piping because of system design, testing, and operational considerations.
- c. The effects of low and high cycle fatigue on the integrity of the primary piping are negligible.
- d. Ample margin exists between the leak rate of small stable flaws and the capability of the H. B. Robinson Unit 2 reactor coolant system pressure boundary Leakage Detection System.
- e. Ample margin exists between the small stable flaw sizes of item d and larger stable flaws.
- f. Ample margin exists in the material properties used to demonstrate end-of-service life (relative to aging) stability of the critical flaws.

For the critical locations, flaws are identified that will be stable because of the ample margins described in d, e, and f above.

Based on the above, the Leak-Before-Break conditions are satisfied for the H. B. Robinson Unit 2 primary loop piping. All the recommended margins are satisfied. It is therefore concluded that dynamic effects of RCS primary loop pipe breaks need not be considered in the structural design basis of the H. B. Robinson Unit 2 Nuclear Power Plant for the License Renewal Program.

APPENDIX A

LIMIT MOMENT

[

face

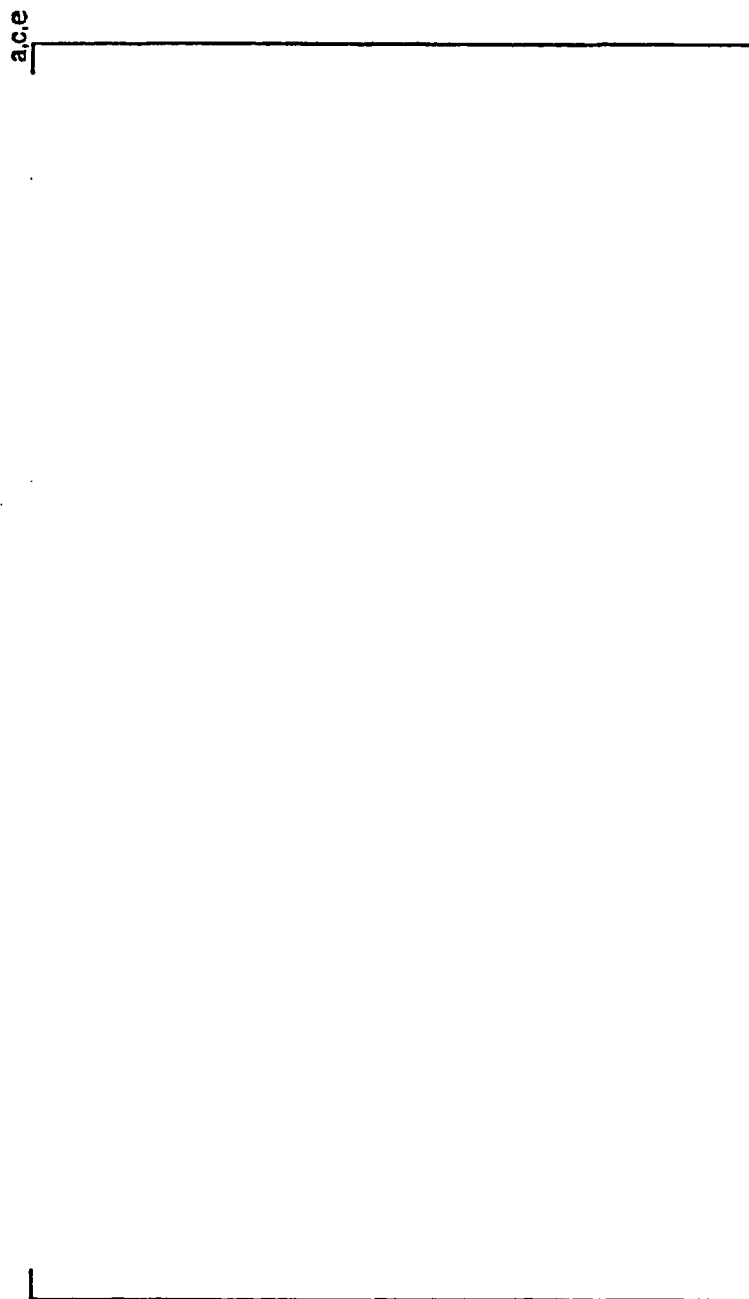


Figure A-1 Pipe with a Through-Wall Crack in Bending